Virology **269,** 190–200 (2000)
doi:10.1006/viro.2000.0212, available online at http://www.idealibrary.com on IDEAL®

Crosslink Analysis of N-Terminal, C-Terminal, and N/B Determining Regions of the Moloney Murine Leukemia Virus Capsid Protein

Jason McDermott,[1] Sonya Karanjia,[1] Zachary Love, and Eric Barklis[2]

Vollum Institute and Department of Microbiology, Oregon Health Sciences University, Portland, Oregon 97201-3098

Received September 15, 1999; returned to author for revision December 10, 1999; accepted January 19, 2000

To analyze contacts made by Moloney murine leukemia virus (M-MuLV) capsid (CA) proteins in immature and mature virus particles, we have employed a cysteine-specific crosslinking approach that permits the identification of retroviral Gag protein interactions at particular residues. For analysis, single cysteine creation mutations were made in the context of protease-deficient or protease-competent parental constructs. Cysteine creation mutations were chosen near the N- and C-termini of CA and at a site adjacent to the M-MuLV Glu-Ala *Fv1* N/B host range determination sequence. Analysis of immature virions showed that PrGag proteins were crosslinked at C-terminal CA residues to form dimers while crosslinking of particle-associated N-terminal and N/B region mutant proteins did not yield dimers, but showed evidence of linking to an unknown 140- to 160-kDa partner. Analysis of mature virions demonstrated that both N- and C-terminal CA residues participated in dimer formation, suggesting that processed CA N- and C-termini are free to establish interprotein associations. Interestingly, N/B region mutant residues in mature virus particles did not crosslink to form dimers, but showed a novel crosslinked band, consistent with an interaction between the N/B tropism determining region and a cellular protein of 45–55 kDa.

INTRODUCTION

The core (Gag) protein of the Moloney murine leukemia virus (M-MuLV) is the primary determinant of virus particle structure and expression of Gag has been shown to be necessary and sufficient for the formation and release of immature virus particles (Craven and Parent, 1996). Gag is synthesized as a myristoylated polyprotein precursor, $Pr65^{Gag}$, which is cleaved by the viral protease (PR) during or after budding to yield the mature viral proteins matrix (MA), p12, capsid (CA), and nucleocapsid (NC) (Barbacid *et al.,* 1976; Bolognesi *et al.,* 1973; Stephenson *et al.,* 1975). The Gag protein is delivered to the plasma membrane by an undetermined mechanism (Swanstrom and Wills, 1997), assembles there, and buds from the cell to yield a roughly spherical virus particle of approximately 125 nm in diameter (Yeager *et al.,* 1998). The MA protein is myristoylated at its N-terminus, associates with membranes, and may interact with the cytoplasmic tail of the viral transmembrane (Env) protein (Swanstrom and Wills, 1997). The role of the p12 domain is not well understood; however, deletion of most of the domain does not substantially affect virus particle assembly (Barklis *et al.,* 1997; Crawford and Goff, 1984). The NC protein specifically binds viral genomic RNA and is required for RNA encapsidation as well as serving a function in the viral assembly process (Campbell and Vogt, 1995; Gorelick *et al.,* 1988; Hansen and Barklis, 1995). The CA domain of M-MuLV has been shown to be important in virus particle assembly (Hansen *et al.,* 1990; Jones *et al.,* 1990; Lobel and Goff, 1984) and budding, as well as playing a role early in infection (Alin and Goff, 1996). Contained in the CA domain are the major homology region (MHR), a region of 20 to 30 residues that is the only highly conserved sequence among retroviral capsid proteins (Craven *et al.,* 1995; Mammano *et al.,* 1994; Strambio-de-Castillia and Hunter, 1992), as well as the N/B locus, the determinant of murine C-type NIH/BALB/c (N/B) cell tropism (Brown, 1997; Weiss *et al.,* 1984).

Although it is clear that mutations in the CA domain can affect M-MuLV particle assembly and release from cells (Hansen *et al.,* 1990; Jones *et al.,* 1990; Lobel and Goff, 1984), the exact role of the CA domain in the assembly process remains largely unknown. Studies on HIV-1 have shown that the carboxyl-terminus of CA is important for virus particle assembly (McDermott *et al.,* 1996; Reicin *et al.,* 1995) but much of the N-terminal portion is dispensable for virus particle assembly (Borsetti *et al.,* 1998; Wang *et al.,* 1994). In Rous sarcoma virus, the essential assembly domains that have been mapped lie outside the CA domain (Swanstrom and Wills, 1997; Weldon and Wills, 1993; Wills *et al.,* 1994). Both the N- and the C-terminal portions of the HIV-1 CA have been crystallized as dimers (Gamble *et al.,* 1997; Momany *et al.,* 1996), and recent biophysical studies

[1] These authors contributed equally to this work.

[2] To whom correspondence and reprint requests should be addressed. E-mail: barklis@ohsu.edu.

0042-6822/00 $35.00

have revealed some details concerning Gag–Gag interactions of HIV-1 (Barklis *et al.,* 1998; Campbell and Rein, 1999; Fuller *et al.,* 1997; Ganser *et al.,* 1999; Scarlata *et al.,* 1998), Rous sarcoma virus (Campbell and Vogt, 1995, 1997; Kovari *et al.,* 1997), and M-MuLV (Barklis *et al.,* 1997; Yeager *et al.,* 1998), but the specific residues involved in interprotein contacts remain to be defined.

As a biochemical approach to examine interactions between CA proteins in M-MuLV, we previously established a system for cysteine crosslinking analysis of proteins in M-MuLV virus particles (Hansen and Barklis, 1995). This system, based on the work of others (Pakula and Simon, 1992; Pepinsky, 1983; Pepinsky *et al.,* 1980; Pinter and Fleissner, 1979), allows cysteine residues that are in close proximity on adjacent proteins to be covalently crosslinked through the addition of cysteine-specific chemical crosslinking reagents such as molecular iodine or bis-maleimido hexane (BMH). Cysteines located on the NC domain in immature (Hansen and Barklis, 1995) and mature (Ott *et al.,* 1998; Rein *et al.,* 1996, 1997) M-MuLV particles were efficiently crosslinked by cysteine-specific crosslinking agents. In addition, we found that mutation of all five cysteines present in M-MuLV Gag was compatible with immature virus particle assembly, allowing us to conveniently examine the effects of cysteine creation mutations in immature virions. In our current study, we also have designed an efficiently processed viral construct, containing no CA or MA cysteine residues, so that CA domain interactions can be probed in mature virus particles.

To probe capsid domain contacts, we have made cysteine creation mutations in three different regions of the M-MuLV CA coding region in both protease-deficient (PR^-) and protease-competent (PR^+) constructs: the N-terminal region of CA (G220C), the C-terminal region of CA (S475C), and the N/B determining region (T323C; see Fig. 1). We observed that in immature virus particles, G220C proteins did not form crosslinked dimers, but S475C proteins did. In contrast, in mature virions, both N- and C-terminally modified proteins crosslinked efficiently to form dimers, suggesting that during viral maturation, the N-terminal portion of CA is reoriented so that it can interact with neighbor molecules. Additionally, cellular proteins of 140–160 and 45–55 kDa were identified as CA crosslinked partners in immature and mature M-MuLV particles, respectively. These proteins may represent cellular factors that actively participate in the M-MuLV replication cycle.

RESULTS

Assembly of immature and mature virus particles

To study M-MuLV virus particle assembly and structure, we have employed a COS cell-based transient transfection system. The vectors used for transfection were based on the parental construct pXM, which carries a simian virus 40 (SV40) origin of replication that allows replication of the plasmid in COS cells, and the adenovirus major late promoter, which fosters high levels of transcription initiation in COS cells. Our parental PR^- construct (pXM2453) deletes M-MuLV *pol* and *env* regions and directs the expression of immature virus particles (Hansen and Barklis, 1995). Our wild-type (wt) construct (pXMGPE) expresses all three M-MuLV genes (*gag, pol,* and *env*) and directs expression of mature M-MuLV particles. Two other parental constructs were employed routinely. These were PR^-Cys^-, which assembles immature virions in which all five *gag* cysteine codons were converted to serines (Fig. 1; Hansen and Barklis, 1995), and MA+$CACys^-$, a PR^+ (pXMGPE) variant in which the MA and CA cysteine codons (Fig. 1) have been converted to serines. Other pertinent mutations were cysteine creation mutations near the N-terminus of the CA domain (G220C), near the CA C-terminus (S475C), and at the N/B determining region (T323C) and a previously studied MHR double mutation, E370C/K373C (Hansen and Barklis, 1995; see Fig. 1). The double mutation was expressed on a PR^-Cys^- background to yield PR^-Cys^- E370C/K373C, while the G220C, S475C, and T323C mutations were expressed in both PR^-Cys^- and MA+$CACys^-$ (but PR^+) contexts, giving PR^-Cys^-G220C, PR^-Cys^-S475C, PR^-Cys^-T323C, MA+$CACys^-$G220C, MA+$CACys^-$S475C, and MA+$CACys^-$T323C.

For assembly analysis, cell lysate and pelleted media supernatant samples were collected 3 days posttransfection, and *gag*-derived proteins were separated by SDS–polyacrylamide gel electrophoresis (SDS–PAGE) and detected by immunoblotting (see Materials and Methods). As can be seen from Fig. 2A, all PR^- constructs were released efficiently from cells as indicated by comparison of $Pr65^{Gag}$ levels in the viral supernatants (Fig. 2A, lanes A–F) versus cell lysates (Fig. 2A, lanes H–M). The PR^+ constructs also directed the efficient release of Gag proteins from cells. As expected (Fig. 2B), wt, MA+$CACys^-$S475C, MA+$CACys^-$T323C, and MA+$CACys^-$G220C $Pr65^{Gag}$ and CA proteins were detected readily in media samples (Fig. 2A, lanes A–D), while only $Pr65^{Gag}$ proteins were observed in cell samples (Fig. 2A, lanes F–I). Note that for the MA+$CACys^-$S475C mutant, a *gag*-derived 40-kDa media band was observed (Fig. 2A, lane B) about 80% of the time with the anti-CA antibodies, Hy187, and the polyclonal anti-CA. Since this band was not observed with the anti-p12 antibody Hy548 in virus particles (data not shown) it may represent an incomplete CA–NC cleavage product. That media supernatant Gag proteins were particle-associated was suggested by the fact that they sedimented through sucrose cushions at clearing rates consistent with sedimentation coefficients of >120S and with densities of 1.15–1.18 g/ml (Hansen and Barklis, 1995; data not shown), as expected for virus particles.

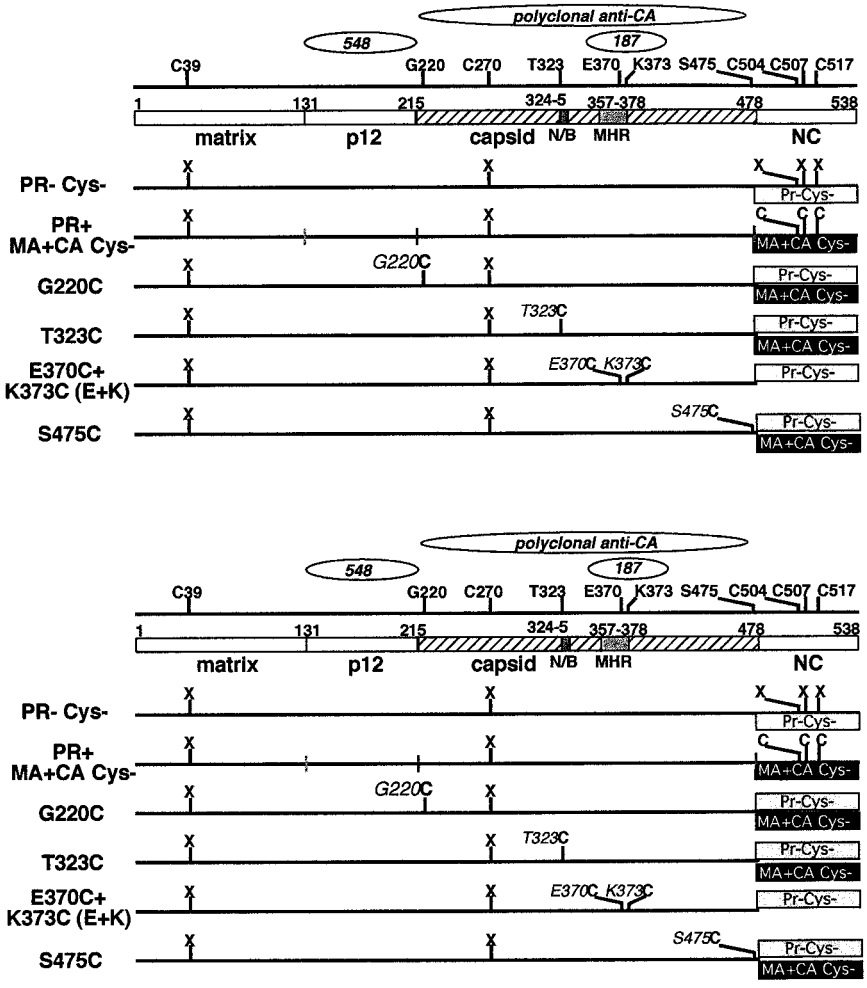

FIG. 1. Schematic diagram of M-MuLV $Pr65^{Gag}$ protein. The M-MuLV $Pr65^{Gag}$ protein consists of four domains, matrix (MA), p12, capsid (CA, stippled lines), and nucleocapsid (NC), that are cleaved by the viral protease (PR) during the budding process. The precursor polypeptide is 538 codons in length and the juncture codons are indicated. The five natural cysteines in $Pr65^{Gag}$ and the five introduced cysteine mutations are indicated on the top bar with their respective *gag* codon numbers. Within the capsid domain, the N/B tropism determination site is at codons 324 and 325 and the MHR includes codons 357 to 378. Antibody epitopes for hybridoma 548, which binds the p12 domain, hybridoma 187, which binds near the MHR, and the polyclonal anti-CA antibody, which binds to the capsid domain, are indicated at the top. Note that the parental immature construct is PR^- and that mutations were constructed on a PR^-Cys^- parent (gray box). In contrast, the mature parent construct eliminated matrix and capsid domain cysteines ($MA+CACys^-$) but retained all NC cysteines (black box). The parental immature and mature constructs as well as the individual cysteine mutations are represented schematically with an X denoting a naturally occurring cysteine that has been removed and a C (preceded by the mutation designation) representing a cysteine creation. Specific cysteine creation mutations use a letter-number-letter nomenclature, where the first letter indicates the wt residue, the number corresponds to the *gag* codon number, and the second letter indicates the newly created amino acid residue. Gray or black boxes associated with each construct denote whether the cysteine creation was expressed in a PR^-Cys^- or $MA+CACys^-$ context or both.

Crosslinking analysis of immature virus particles

To test the proximity of CA domain cysteine residues in Pr^{Gag} proteins in immature M-MuLV virus particles we utilized our established crosslinking protocol (Hansen and Barklis, 1995; McDermott *et al.,* 1996). Briefly, unique cysteine residues on adjacent molecules will not form covalent crosslinks if the cysteine residues are separated by too great a distance, when treated with membrane-permeable, cysteine-specific crosslinking agents such as molecular iodine (maximum crosslinking distance approximately 5 Å) or BMH (maximum crosslinking distance approximately 15 Å). In contrast, adjacent molecules with cysteines in close proximity may form covalent crosslinks that can be detected after gel electrophoresis and immunoblotting. As shown in Fig. 3, when PR^- virions lacking both *pol* and *env* gene products were mock-treated, the expected $Pr65^{Gag}$ band was detected with anti-p12 antibodies (Fig. 3, lane F). However, a parallel crosslinked sample (Fig. 3, lane E) gave the 65-kDa band plus a 130-kDa dimer product, consistent with previous observations (Hansen and Barklis, 1995), demonstrating $Pr65^{Gag}$ crosslinking via NC cysteine residues. As expected, crosslinking treatment of the PR^-Cys^- mutant particles showed only a trace of a band

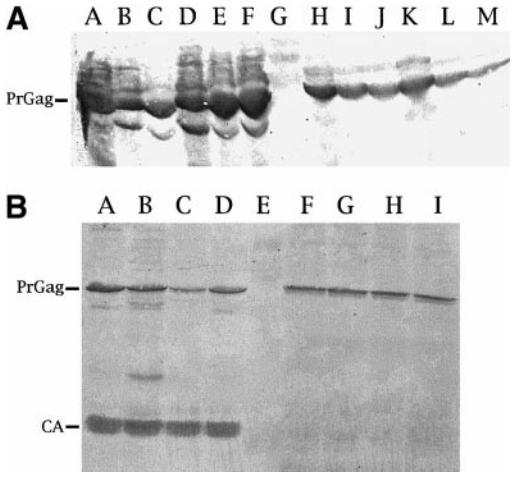

FIG. 2. Expression and release of mutant Gag proteins. (A) As described under Materials and Methods, virus particle (lanes A–F) and cell lysate (lanes H–M) samples were collected from cells transfected with the following PR$^-$ pXM2453 vectors: wt PR$^-$ (lanes A, H), PR$^-$Cys$^-$ (B, I), PR$^-$Cys$^-$E370C/K373C (C, J), PR$^-$Cys$^-$G220C (D, K), PR$^-$Cys$^-$S475C (E, L), PR$^-$Cys$^-$T323C (F, M). Samples were subjected to SDS–PAGE and electroblotted, and Gag proteins were detected with the anti-p12 antibody Hy548. The protein size standard (faint) is in lane G, and the Pr65^{Gag} band is indicated. (B) Virus particle (lanes A–D) and cell lysate (lanes F–I) samples were collected from cells transfected with the following pXMGPE (PR$^+$) vectors: wt (lanes A, F), MA+CACys$^-$S475C (B, G), MA+CACys$^-$T323C (C, H), MA+CACys$^-$G220C (D, I). Samples were fractionated and immunoblotted as above, except the anti-CA antibody Hy187 was employed. The protein size standard appears faintly in lane E, and Pr65^{Gag} and CA proteins are as indicated.

at 130 kDa (Fig. 3, lane C; discussed below), consistent with the specificity of BMH for preferential crosslinking at cysteine residues. Results from crosslinking treatments of PR$^-$Cys$^-$E370C/K373C particles also agreed with previous results, showing no dimer band, but instead a crosslinked product at about 190 kDa (Fig. 3, lane A). Neither the N-terminal PR$^-$Cys$^-$G220C nor the PR$^-$Cys$^-$T323C mutant particles gave Pr65^{Gag} dimer bands upon crosslinking (Fig. 3, lanes I and K), but each showed crosslinked bands at 190 kDa, similar to that seen for PR$^-$Cys$^-$E370C/K373C. In contrast, crosslinking of PR$^-$Cys$^-$S475C particles, which carry single Pr65^{Gag} cysteines near the C-terminus of the CA domain, gave a band that comigrates with Pr65^{Gag} dimers (Fig. 3, lane G), suggesting that C-terminal CA domains are in close proximity in immature M-MuLV virions.

Although the results shown in Fig. 3 were observed in almost all experiments, it is important to point out that experiment-to-experiment variations were observed. While PR$^-$ showed Pr65^{Gag} crosslinked dimers in 18 of 18 experiments with three different antibodies (Table 1), it also showed evidence of a 190-kDa band at least once. As noted above, a faint dimer band was seen on BMH treatment of PR$^-$Cys$^-$ particles (Fig. 3, lane C). Faint dimers were observed in 36% of our experiments using two different antibodies: we assume that such dimers resulted from maleimide side reaction with histidines and primary amine groups, which can occur at low levels at pH 7.4–7.5 (Smyth *et al.,* 1964). We also observed some crosslinking variability with PR$^-$Cys$^-$G220C, PR$^-$Cys$^-$T323C, PR$^-$Cys$^-$E370C/K373C, and PR$^-$Cys$^-$S475C particles (Table 1). However, the general conclusions of Fig. 3 were supported in multiple experiments. Specifically, the PR$^-$Cys$^-$S475C mutant proteins showed 130-kDa bands 91% of the time, while the PR$^-$Cys$^-$G220C, PR$^-$Cys$^-$T323C, and PR$^-$Cys$^-$E370C/K373C mutants gave 190-kDa bands 93, 82, and 100% of the time, respectively. A crosslinked band of this size could represent a Gag protein crosslinked to a cellular protein or, alternatively, a crosslinked Gag trimer, which seems unlikely since the band is observed with mutant Gag proteins containing only one cysteine residue.

Crosslinking analysis of mature virus particles

For crosslinking studies on mature virus particles, we employed a parental MA+CA cysteine to serine construct (MA+CACys$^-$), which does not block proteolytic processing. The experimental methods used for crosslinking analysis of mature virus particles followed those used for the immature virus particles (see above). As shown in Fig. 4, proteins from MA+CACys$^-$ particles showed only Pr65^{Gag} and CA bands but no crosslinked bands (Fig. 4, lanes A and B) as expected. With mock-treated MA+CACys$^-$G220C a 58-kDa band was observed in addition to the Pr65^{Gag} and CA bands (Fig. 4,

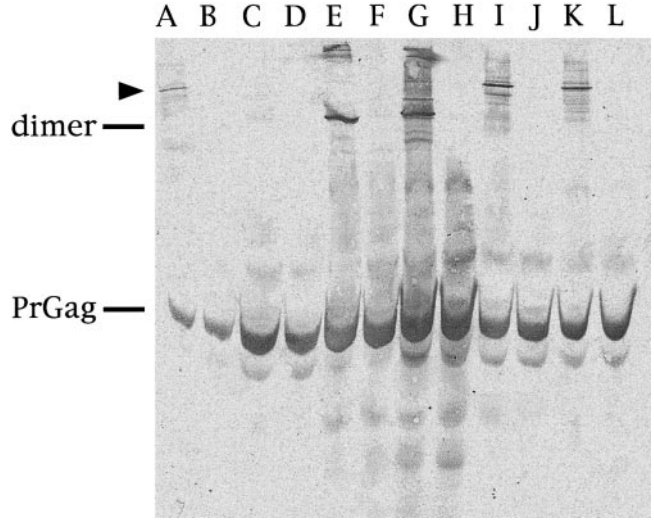

FIG. 3. Crosslinking of M-MuLV protease-minus Gag proteins. Immature virus particles produced by constructs PR$^-$Cys$^-$E370C/K373C (lanes A, B), PR$^-$Cys$^-$ (C, D), PR$^-$ (E, F), PR$^-$Cys$^-$S475C (G, H), PR$^-$Cys$^-$G220C (I, J), and PR$^-$Cys$^-$T323C (K, L) were mock-treated (lanes B, D, F, H, J, and L) or treated with BMH (lanes A, C, E, G, I, and K), as described under Materials and Methods, to crosslink neighboring cysteine residues. Samples were subjected to SDS–PAGE and electroblotted, and Gag proteins were detected with the anti-p12 antibody Hy548. Pr65^{Gag} proteins and the putative Pr65^{Gag} homodimers are indicated. The arrow denotes the putative heterodimer crosslinked band for lanes A, I, and K.

TABLE 1

Observed Crosslinked Bands for PR$^-$ Constructs

Construct	Crosslinked band	% time observed	Total no. gels	Antibodies
PR$^-$	PrGag dimer	100	18	187, 548, CA
	PrGag tetramer	17	18	187, 548, CA
	220 kDa	6	18	548
	205 kDa	6	18	548
	190 kDa	6	18	548
PR$^-$Cys$^-$	PrGag dimer (faint)	36	14	548, CA
	190 kDa	14	14	548
	160 kDa	7	14	CA
PR$^-$Cys$^-$E370C/K373C	PrGag dimer	7	14	CA
	190 kDa	93	14	548, CA
PR$^-$Cys$^-$G220C	PrGag dimer	9	11	548
	190 kDa	82	11	187, 548
PR$^-$Cys$^-$S478C	PrGag dimer	91	11	187, 548
	190 kDa	9	11	548
PR$^-$Cys$^-$T323C	PrGag dimer	0	8	548
	190 kDa	100	8	548

Note. Crosslinking reactions were performed as described under Materials and Methods on immature virus particles produced on transfection of cells with the indicated constructs. Crosslinked bands are designated as putative Pr^{Gag} dimers or tetramers or as apparent molecular masses of crosslinked species. The designation of "faint" for PR$^-$Cys$^-$ Pr^{Gag} dimers indicates that bands were detectable, but at levels less than 10–25% of wt Pr^{Gag} dimers. The total number of gels signifies the number of independent crosslinking experiments; the percentage of time observed is based on the total number of gels. The antibodies column indicates the different antibodies that have been used to detect a specific crosslinked band.

lane C). Since this band also was detected with our anti-p12 antibody (Hy548; Fig. 4, lane E) it is possible that the band represents a processing intermediate and may comprise the MA+p12+CA domains. Notwithstanding the putative processing intermediate, examination of the crosslinked G220C sample showed an additional 60-kDa band (Fig. 4, lane D), consistent with the creation of a CA–CA crosslink dimer. As would be expected for a strictly CA-derived moiety, the 60-kDa band was not detected with the anti-p12 antibody (Fig. 4, lane F), supporting the notion that the band corresponds to a CA–CA dimer. In the case of the MA+CACys$^-$S475C mutant, we observed the faint uncrosslinked 40-kDa band (Fig. 4, lane G), which appears to correspond to a CA–NC processing intermediate (as in Fig. 2). In Fig. 4, lane H, an additional crosslinked band at 62 kDa was observed. This 62-kDa band was not detected with the anti-p12 Hy548 antibody (data not shown), suggesting that it also

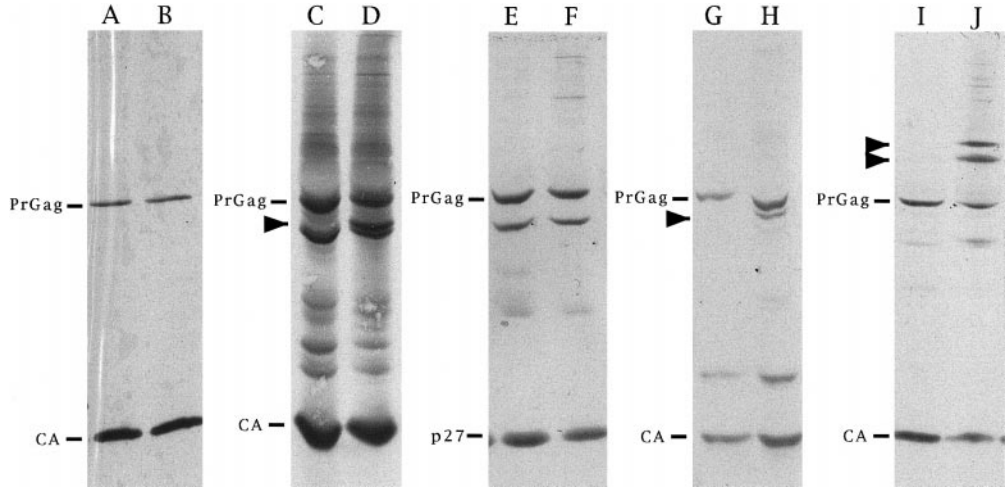

FIG. 4. Crosslinking of mature M-MuLV Gag proteins. Virus particles from cells transfected with pXMGPE (wild type; A, B), MA+CACys$^-$G220C (C–F), MA+CACys$^-$S475C (G, H), and MA+CACys$^-$T323C (I, J) were mock-treated (lanes A, C, E, G, and I) or treated with BMH (lanes B, D, F, H, and J) as described under Materials and Methods. Protein samples were fractionated by SDS–PAGE, electroblotted, and then detected with the anti-CA hybridoma Hy187 (lanes A–D, G–J) or the anti-p12 hybridoma Hy548 (lanes E, F). Bands corresponding to Pr65Gag, CA, and the proteolytic MA+p12 fragment p27 are indicated. Arrows in lanes D, H, and J indicate crosslinked bands.

TABLE 2

Observed Crosslinked Bands for PR^+ Constructs

Construct	Crosslinked band	% time observed	Total no. gels	Antibodies
wt	PrGag dimer	40	25	187, 548, CA
	60 kDa	8	25	187
	62 kDa	4	25	187
	37 kDa	4	25	187
MA+CACys⁻G220C	PrGag dimer	15	27	187, 548, CA
	60 kDa	89	27	187, CA
	75 kDa	4	27	187
	40 kDa	4	27	187
MA+CACys⁻S478C	PrGag dimer	9	22	187, 548
	62 kDa	64	22	187
	60 kDa	27	22	187
	45 kDa	18	22	187
	75 kDa	9	22	187
	40 kDa	9	22	187
	37 kDa	5	22	187
MA+CACys⁻T323C	PrGag dimer	4	25	187
	80 kDa	76	25	187
	75 kDa	76	25	187
	60 kDa	24	25	187
	50 kDa	4	25	187

Note. Crosslinking reactions were performed as described under Materials and Methods on mature virus particles produced on transfection of cells with the indicated constructs. Crosslinked bands are designated as putative PrGag dimers and as apparent molecular masses of crosslinked species. The total number of gels signifies the number of independent crosslinking experiments; the percentage time observed is based on the total number of gels. The antibodies column indicates the different antibodies that have been used to detect a specific crosslinked band.

represents a CA–CA dimer, which migrates slightly differently than the apparent G220C CA–CA dimer, possibly because of its different crosslinking site. While the MA+CACys⁻G220C and S475C variants showed putative CA crosslinked dimer bands, the MA+CACys⁻T323C crosslinking pattern was quite different. As shown (Fig. 4, lane J), a faint 60-kDa dimer may be evident, but the prominent crosslinked bands migrated at 75 and 80 kDa (arrows).

As with the PR^- crosslinking results (Fig. 3; Table 1), although the crosslinking results with mature virus particles were generally reproducible, some variability was observed (Table 2). Nevertheless, with the MA+CACys⁻G220C mutant, the 60-kDa putative dimer band was observed nearly 90% of the time. While less consistent, the putative MA+CACys⁻S475C CA dimers were observed nearly two-thirds of the time, and MA+CACys⁻T323C 75- to 80-kDa bands were seen in three-quarters of the experiments. In contrast, with the wt construct, 60-, 62-, 75-, and 80-kDa bands were observed less than 10% of the time (Table 2).

Both the 75- and the 80-kDa crosslinked bands were observed after iodine-mediated crosslinking (data not shown), supporting the notion that interacting cysteines were close enough to form disulfides. During follow-up studies with reducible cysteine-specific crosslinking agents, we found that formation of reducible Gag protein crosslinks could be induced simply by particle treatment with dimethyl sulfoxide (DMSO), which often is used to solubilize membrane-permeant crosslinking agents. The crosslinking potential of DMSO has been reported previously (Tam *et al.,* 1991) and is consistent with reports of its oxidizing capabilities. To ascertain DMSO crosslinking effects on mature virions, particles were treated with DMSO and then either reduced (Fig. 5, lanes A to D) or not reduced (Fig. 5, lanes E to H), fractionated by SDS–PAGE, and immunoblotted to detect Gag proteins. For wt M-MuLV mature virus particles, no crosslinking was detected with DMSO (compare Fig. 5, lanes A and E), as expected from BMH results (Fig. 4) and indicating that

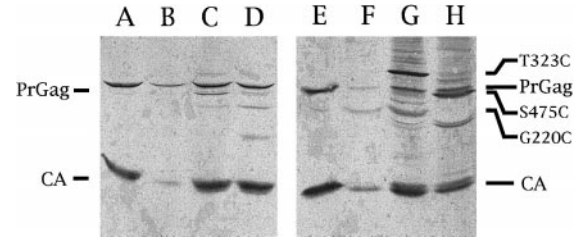

FIG. 5. DMSO-induced crosslinking of mature virus particle proteins. Virus particles from cells transfected with pXMGPE (wild type; A, E), MA+CACys⁻G220C (B, F), MA+CACys⁻T323C (C, G), and MA+CACys⁻S475C (D, H) were treated with DMSO as described under Materials and Methods. Protein samples were separated on a reducing gel (lanes A–D) or a nonreducing gel (lanes E–H), after which electroblotted Gag proteins were detected using the anti-CA antibody Hy187. Bands representing the $Pr65^{Gag}$ and mature CA proteins are indicated, as are the locations of the crosslinked products for each mutant at the right.

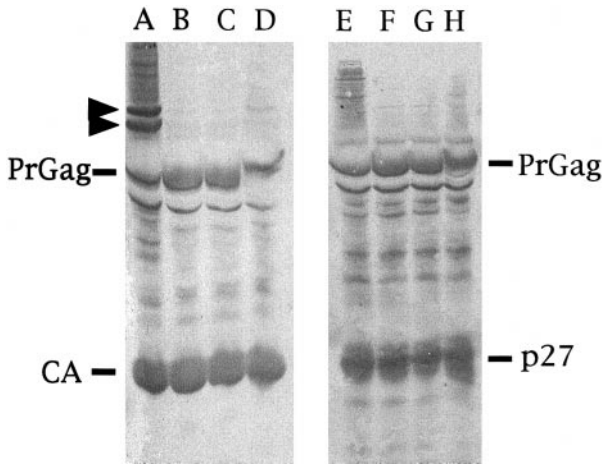

FIG. 6. Composition of the MA+CACys$^-$T323C crosslinked band. Virus particles from cells transfected with MA+CACys$^-$T323C were either BMH-treated (A, E) or mock-treated (B–D, F–H), after which protein samples were fractionated on a reducing SDS–PAGE gel. After electrophoresis, samples were electroblotted and then immunoblotted using either the anti-CA antibody, Hy187 (lanes A–D), or the anti-p12 antibody, Hy548 (lanes E–H). Indicated are Pr65^{Gag}, CA, and the proteolytic MA+p12 fragment, p27. Arrows indicate the 75- and 80-kDa crosslinked bands.

the natural capsid cysteine residues (C270; Fig. 1) are not in close proximity on neighbor molecules. In contrast to the wt results, but in concert with comparable BMH results (Fig. 4), MA+CACys$^-$G220C proteins showed the putative CA dimer band at 60 kDa (Fig. 5, lane F) and putative 62-kDa MA+CACys$^-$S475C dimer bands were also observed (Fig. 5, lane H). Furthermore, one CA crosslinked band was present at 75–80 kDa in the treated MA+CACys$^-$T323C mutant lane (Fig. 5, lane G), consistent with the appearance of a single 80-kDa crosslinked product or the comigration of the 75- and 80-kDa species seen in Fig. 4. From these data it appears that MA+CACys$^-$G220C, T323C, and S475C crosslinking partners are within 5 Å of one another. Since BMH samples were run under reducing conditions (Figs. 3 and 4), it also would appear that BMH reacts with cysteines more quickly than its solvent, DMSO, or that DMSO-induced disulfides can exchange with BMH to form nonreducible crosslinks.

Based on the size of the MA+CACys$^-$T323C crosslinked bands and amounts of Pr65^{Gag} present in virus particle preparations, it was possible that the 75- to 80-kDa bands could represent fast-migrating crosslinked Pr65^{Gag}-CA species. To test this hypothesis, MA+CACys$^-$T323C controls (Fig. 6, lanes B–D and F–G) and BMH crosslinked samples (Fig. 6, lanes A and E) were electrophoresed and blotted in parallel with anti-CA antibody (Hy187; Fig. 6, lanes A–D) or with anti-p12 antibody (Hy548; Fig. 6, lanes E–H). The 75- and 80-kDa bands were detected with the anti-CA antibody but not the anti-p12 antibody (Fig. 6, lane A versus lane E), indicating that the 75- and 80-kDa bands were not derived from Pr65^{Gag} crosslinks. We also performed parallel crosslinking immunoblots with anti-actin, anti-tubulin, and anti-PDI (protein disulfide isomerase) antibodies. These experiments were performed because HIV-1 Gag proteins have been shown to interact with cytoskeletal proteins (Ott *et al.,* 1996; Perrin-Tricaud *et al.,* 1999; Rey *et al.,* 1996; Wilk *et al.,* 1999), while PDI, which catalyzes protein disulfide formation and exchange, could be postulated to associate with cysteine residues on mutant proteins. Nevertheless, actin, tubulin, and PDI antibodies did not bind to the 75- to 80-kDa MA+CACys$^-$T323C crosslinked bands (data not shown), suggesting the existence of alternate crosslinked partners in these virions.

DISCUSSION

In this paper, we describe the crosslinking analysis of M-MuLV capsid proteins in mature and immature virus particles. These experiments were undertaken to complement structural models derived from *in vitro* studies. Although previous crosslinking studies have been employed successfully to examine viral protein interactions (Pepinsky, 1983; Pepinsky *et al.,* 1980; Pinter and Fleissner, 1979), we chose the cysteine crosslinking approach to avoid complications in interpretation arising from using amine-specific crosslinking agents, which can react with a large number of residues present in M-MuLV Gag. Nevertheless, as with other crosslinking methods, the composition of crosslinked bands has been inferred from gel mobilities, and interpretations must be considered with this caveat in mind. Because our approach requires making mutations on PR$^-$Cys$^-$ and MA+CACys$^-$ parental constructs, some results may not be pertinent wt constructs. Additionally, the PR$^-$ construct does not express *pol* and *env* gene products, an alteration that may disrupt the internal structure of immature virions. Since we have not performed electron microscope analyses of virus particles produced from transiently transfected cells, we do not know whether some mutants might show morphologies that are visibly different from their wt counterparts. However, the PR$^-$Cys$^-$ and MA+CACys$^-$ Gag proteins directed the efficient assembly of particles with apparently normal masses and densities (Fig. 2; Hansen and Barklis, 1995; data not shown), and the approach has been used previously to examine retrovirus particle structures (Hansen and Barklis, 1995; McDermott *et al.,* 1996). Thus, we believe that our results are relevant to the analysis of immature and mature M-MuLV particles.

Our studies show that particle-associated wt PR$^-$ Gag proteins can be crosslinked to form dimers (Fig. 3). This finding is consistent with our previous observations that Pr^{Gag} proteins in immature virions crosslink via the NC zinc finger cysteines (Hansen and Barklis, 1995) and agrees with the previous results showing that NC cysteines are targets for thiol reactive compounds (Ott *et al.,*

1998; Rein *et al.,* 1996, 1997). We also observed that PR$^-$Cys$^-$S475C proteins could be crosslinked to form dimers, suggesting that CA C-terminal domains are closely associated in immature virions. In contrast, Pr65^{Gag} dimers were not observed with the PR$^-$Cys$^-$G220C, T323C, or E370C/K373C mutants (Fig. 3). Instead crosslinked bands from these mutants migrated with apparent mobilities of 185–190 kDa on 7.5% gels, similar to our previous observations for the PR$^-$Cys$^-$E370C/K373C mutant (Hansen and Barklis, 1995), as well as for the other major homology region mutants PR$^-$Cys$^-$L369C and PR$^-$Cys$^-$E370C (Hansen and Barklis, 1995). The observed 190-kDa band is approximately the size of three covalently linked Pr^{Gag} monomers, but is seen with mutants containing only one cysteine residue. This consideration is consistent with the crosslinking partner being a cellular protein or with anomalous crosslinking of Pr^{Gag} monomers to form trimers. We are attempting to generate a sufficient quantity of the 190-kDa band to characterize this complex further.

Relative to immature virions, CA proteins in mature M-MuLV particles showed different crosslinking reactivities. While the natural CA C270 residues did not mediate dimer formation in mature virions (Fig. 4), BMH (Fig. 4), iodine (data not shown), and DMSO (Fig. 5) treatments yielded both MA+CACys$^-$G220C and S475C 60- to 62-kDa crosslinked bands, which appear to correspond to CA–CA dimers. Assuming that the 60- to 62-kDa bands represent bona fide CA dimers, our results suggest that during maturation, capsid protein interactions reorganize to permit dimer formation at both N- and C-termini. This is consistent with the maturational conformation model proposed for HIV-1 in which constrained Pr^{Gag} CA N-termini refold during proteolytic processing (Schwedler *et al.,* 1998) and previous crosslinking results in M-MuLV (Pepinsky, 1983) and in avian sarcoma and leukemia viruses (Pepinsky *et al.,* 1980). Structural studies on HIV-1 and EIAV have shown that these capsid proteins crystallize as dimers (Gamble *et al.,* 1997; Jin *et al.,* 1999; Momany *et al.,* 1996) with higher order interactions forming the supermolecular particle structure. Our data support the idea that multiple and distant regions of the M-MuLV capsid domain participate in close interprotein contacts in both the immature and the mature virus particle structures.

In contrast to results with MA+CACys$^-$G220C and S475C, the 75- to 80-kDa T323C crosslinked products do not appear to be simple CA dimers. Our evidence suggests that the 75- to 80-kDa bands contain a CA moiety, but do not appear to be composed of p12-containing Pr^{Gag} molecules (Fig. 6). Conceivably, these bands could represent anomalously migrating CA trimer bands, but crosslinked trimers are unexpected for monomers, which carry only single cysteines. Based on parallel immunoblot analysis, the MA+CACys$^-$T323C crosslinked partners do not appear to be actin, tubulin, or PDI. Furthermore the 75- to 80-kDa products would seem to be too small to include *env* gene product, gp70, or viral reverse transcriptase proteins. It is intriguing to speculate whether the MA+CACys$^-$T323C crosslinked partner could be involved in the *Fv1* host-range restriction phenomenon. In this regard, it is of interest that the predicted size of the *Fv1* N/B-related murine host factor is about 52 kDa and appears to correspond to a murine homolog of the *gag* gene of the human endogenous retrovirus, HERV-L (Best *et al.,* 1996). However, while the 75- to 80-kDa MA+CACys$^-$T323C crosslinked products suggest that crosslinked partners are present at reasonably high levels in virus particles produced from African green monkey (COS) cells, the Fv1 gene product appears to exert its effects in target murine cells, despite very low levels of expression (Best *et al.,* 1996). Consequently, for the present it is not clear how or if the MA+CACys$^-$T323C crosslinked partners relate to *Fv1* restriction.

MATERIALS AND METHODS

Constructs

The M-MuLV transient expression vector was derived from pXM (Yang *et al.,* 1986), which uses an SV40 origin of replication and adenovirus major late promoter. Construction and sequencing of mutant vectors followed standard protocols (Maniatis *et al.,* 1982). M-MuLV was modified by the addition of 5′ *Eco*RI and *Eco*RV sites (GAATTCGATATCAAGCTT) at the *Hin*dIII site [M-MuLV nt 563 (Shinnick *et al.,* 1981)] of pMov-Psi (Mann *et al.,* 1983) and used to create pXMGPE, which spans M-MuLV nt 566 to 7846 and expresses M-MuLV *gag, pol,* and *env* gene products. The PR$^-$ transient expression vector pXM2453 encodes M-MuLV viral nt 566–2453 and has a termination signal downstream of nt 2453 and thus lacks both the *pol* and the *env* genes. Downstream junction sequences for both constructs are as follows: pXMGPE, 5′ TTTGGCAAGCTAGA 3′, in which nt 7840 from the 3′ untranslated sequence is underlined; pXM2453, 5′ GGT AAG GTC ACC GCG GAT CCC CCT **TAA** GTT AAC TTA AGG GCT GCA GGA ATT C 3′, in which nt 2453 is underlined and the termination codon is in boldface type. As previously described (Hansen and Barklis, 1995), pXMGPE and pXM2453 were used as PR$^+$ and PR$^-$ templates for the introduction of cysteine-to-serine point mutations. All five cysteine-to-serine point mutations, including C504S/C507S, previously described (Gorelick *et al.,* 1988), were cloned into the two parental vectors to yield a pXM2453 all cysteine-to-serine construct (pXM2453Cys$^-$ or PR$^-$Cys$^-$) and a pXMGPE all cysteine-to-serine construct (pXMGPECys$^-$ or wtCys$^-$). The sequences of these cysteine mutants, with the first nucleotide of the sequence listed, the modified nucleotides in boldface type, and the codons where an amino acid was changed underlined, are as follows: C39S (nt 723), 5′

TGG GTT AC**G** TTC TCC T**C**T GCA 3′; C270S (nt 1419), 5′ TGG GAC GA**T** A**G**T CAA CAG 3′; C504S/C507S (nt 2123), 5′ GAC CAG T**C**T GCC TAC T**C**C AAA 3′; and C517S (nt 2163), 5′ AAA GAT T**C**T CCC AAG AA**G** CC**T** CGA 3′. In addition to the pXMGPE Cys^- construct, we constructed a pXMGPE capsid cysteine-to-serine construct (pXMGPECACys^- or CACys^-), which contains only the C270S mutation. Additionally, a pXMGPE matrix plus capsid cysteine-to-serine construct (pXMGPEMA+CACys^- or MA+CACys^-), which contains the C39S and C270S mutations, was also made.

With regard to cysteine creation mutants, PR^-Cys^-E370C/K373C, has been described (Hansen and Barklis, 1995). It introduces two cysteine residues in the MHR region (E370C/K373C [nt 1722], 5′ TTC CTA **TGT C**GA CTT **TGC** GAA GCC TAT CGC ACG TAC ACT CC**A** TAT 3′). In addition to this cysteine creation mutant, several others were made in the capsid domain: G220C (shown from nt 1266), 5′ CCC CTC CGC GCA **TG**C GGA AAC GGA 3′; T323C (shown from nt 1566), 5′ CGC CCA GAC **A**GG GAT TAC ACA **TGT** CCC AGG 3′; and S475C (shown from nt 2031), 5′ CAT AGA GAG ATG **TG**T AAG CTA TTG GCC 3′. These mutants were introduced into the parental constructs PR^-Cys^-, CACys^-, and MA+CACys^-.

Cell culture and viruses

COS1 and COS7 cells were maintained in Dulbecco's modified Eagle's medium (DMEM) supplemented with 10% heat-inactivated fetal calf serum, penicillin, and streptomycin. Cells were split 1:4 from confluent plates onto 10-cm-diameter plates 24 h prior to transfections and were transfected with 16 μg plasmid DNA by the calcium phosphate precipitation method (Hansen and Barklis, 1995). Three days posttransfection, cell lysates and supernatants were collected as previously described (Hansen and Barklis, 1995). Cell-free supernatants from transfected cells were centrifuged through 4-ml 20% sucrose cushions at 83,000 *g* (25,000 rpm in an SW28 rotor) for 2 h at 4°C. Virus pellets were resuspended in phosphate-buffered saline [PBS; 9.5 mM sodium potassium phosphate (pH 7.4), 137 mM NaCl, 2.7 mM KCl]. Cells were rinsed twice with PBS, collected in IPB [20 mM Tris–hydrochloride (pH 7.5), 150 mM NaCl, 1 mM EDTA, 0.1% SDS, 0.5% sodium deoxycholate, 1% Triton X-100, 0.02% sodium azide], vortexed for 1 min, and centrifuged (13,700 *g,* 4°C, 10 min) to remove insoluble material. For protein gels, solubilized cellular lysates were mixed with equal volumes of 2× sample buffer [12.5 mM Tris–hydrochloride (pH 6.8), 2% SDS, 20% glycerol, 0.25% bromophenol blue] plus 5% β-mercaptoethanol (β-Me).

Sucrose density gradient fractionation of virus particles was performed as previously described (Hansen and Barklis, 1995; McDermott *et al.,* 1996). Briefly, extracellular virions were isolated by pelleting through sucrose cushions as described above, after which they were applied to sucrose gradients consisting of 1.1-ml layers of 20, 30, 40, and 50% sucrose that had been allowed to mix by sitting for 1 h at 4°C. Gradients were centrifuged at 300,000 *g* (50,000 rpm in an SW50.1 rotor) overnight at 4°C and 400-μl fractions were collected from top to bottom for analysis by immunoblotting as described below.

Protein and crosslinking analysis

Protein samples were analyzed by SDS–PAGE (Laemmli, 1970). Unless otherwise stated, electrophoresis was performed using 7.5 or 10% SDS–PAGE gels. Electrophoresis ordinarily was performed under reducing conditions, which were achieved by the addition of an equal volume of 2× sample buffer plus 5% β-Me (v/v Final) to the protein samples. For nonreducing conditions, β-Me was omitted. After electrophoresis under standard conditions (Hansen *et al.,* 1990, 1993; Hansen and Barklis, 1995; Jones *et al.,* 1990; Laemmli, 1970; McDermott *et al.,* 1996), gels were electroblotted onto nitrocellulose filters and proteins were detected using the Western blot procedure previously described (Hansen and Barklis, 1995). For size estimates, mobilities were plotted versus log molecular weights of known size standards. For immunoblotting, primary antibodies used were rat monoclonal antibody hybridoma cell supernatants anti-M-MuLV $p12^{Gag}$ (Hy548) and anti-M-MuLV $p30^{Gag}$ (Hy187) used at 1:10 dilutions (Chesebro *et al.,* 1983); polyclonal goat anti-M-MuLV $p30^{Gag}$ (National Cancer Institute), used at a 1:4000 dilution; mouse monoclonal anti-actin antibody (Boehringer Mannheim) used at 1:2000 dilution; mouse monoclonal anti-protein disulfide isomerase (PDI; Affinity Bioreagents, Inc.) used at a dilution of 1:2000, and mouse monoclonal anti-tubulin (Amersham) used at a dilution of 1:200. Secondary alkaline phosphatase-conjugated antibodies were goat anti-mouse immunoglobulin G (IgG; Promega) used at a 1:20,000 dilution and rabbit anti-goat IgG (Boehringer Mannheim), used at a 1:10,000 dilution.

Iodine crosslinking of cysteine residues was performed as previously described (Hansen *et al.,* 1993; Pakula and Simon, 1992) and analyzed by nonreducing SDS–PAGE. For cross-linking with BMH (Pierce), BMH was prepared fresh as a 100 mM solution in DMSO (Mallinckrodt). Viral samples were split into equivalent 100-μl fractions, treated with BMH (1 μl of 100 mM BMH in DMSO) or mock-treated (1 μl of DMSO), vortexed gently, and incubated at room temperature for 1 h. Reactions were terminated by the addition of 2× sample buffer plus β-Me to 5%, and the samples were boiled for 3–5 min. For DMSO oxidation treatments (Tam *et al.,* 1991), 1 μl of DMSO was added to each 100-μl tube, vortexed gently, and incubated at room temperature. Reac-

tions were terminated by the addition of 2× sample buffer without B-Me followed by sample boiling for 3–5 min.

ACKNOWLEDGMENTS

We are grateful for the help and advice provided to us by Haoyu Qian, Marylene Mougel, Guy Zuber, and Katie Poptart Brown. This work was funded by a grant (5 RO1 GM52914-05) from the National Institute of General Medical Sciences (NIGMS).

REFERENCES

Alin, K., and Goff, S. P. (1996). Amino acid substitutions in the CA protein of Moloney murine leukemia virus that block early events in infection. *Virology* **222,** 339–351.

Barbacid, M. J., Stephenson, J., and Aaronson, S. (1976). Gag gene of mammalian type-C RNA tumor viruses. *Nature* **262,** 554–559.

Barklis, E., McDermott, J., Wilkens, S., Fuller, S., and Thompson, D. (1998). Organization of HIV-1 capsid proteins on a lipid monolayer. *J. Biol. Chem.* **273**(13), 7177–7180.

Barklis, E., McDermott, J., Wilkens, S., Schabtach, E., Schmid, M. F., Fuller, S., Karanjia, S., Love, Z., Jones, R., Rui, Y., Zhao, X., and Thompson, D. (1997). Structural analysis of membrane-bound retrovirus capsid proteins. *EMBO J.* **16**(6), 1199–1213.

Best, S., Tissier, P. L., Towers, G., and Stoye, J. P. (1996). Positional cloning of the mouse retrovirus restriction gene *Fv1*. *Nature* **382**(6594), 826–829.

Bolognesi, R. D., Luftig, R., and Shaper, J. (1973). Localization of RNA tumor virus polypeptides. I. Isolation of further virus substructures. *Virology* **56,** 549–564.

Borsetti, A., Ohagen, A., and Gottlinger, H. G. (1998). The C-terminal half of the human immunodeficiency virus type 1 Gag precursor is sufficient for efficient particle assembly. *J. Virol.* **72**(11), 9313–9317.

Brown, P. O. (1997). Integration. *In* "Retroviruses" (J. M. Coffin, S. H. Hughes, and H. E. Varmus, Eds.), pp. 161–203. Cold Spring Harbor Laboratory Press, Plainview, NY.

Campbell, S., and Rein, A. (1999). In vitro assembly properties of human immunodeficiency virus type 1 Gag protein lacking the p6 domain. *J. Virol.* **73**(3), 2270–2279.

Campbell, S., and Vogt, V. (1995). Self-assembly in vitro of purified CA-NC proteins from Rous sarcoma virus and human immunodeficiency virus type 1. *J. Virol.* **69**(10), 6487–6497.

Campbell, S., and Vogt, V. M. (1997). In vitro assembly of virus-like particles with Rous sarcoma virus Gag deletion mutants: Identification of the p10 domain as a morphological determinant in the formation of spherical particles. *J. Virol.* **71**(6), 4425–4435.

Chesebro, B., Britt, W., Evans, L., Wehrly, K., Nishio, J., and Cloyd, M. (1983). Characterization of monoclonal antibodies reactive with murine leukemia viruses: Use in analysis of strains of Friend MCF and Friend ecotropic murine leukemia virus. *Virology* **127,** 134–148.

Craven, R. C., Leure-duPree, A. E., Weldon, R. A., and Wills, J. W. (1995). Genetic analysis of the major homology region of the Rous sarcoma virus Gag protein. *J. Virol.* **69,** 4213–4227.

Craven, R. C., and Parent, L. J. (1996). Dynamic interactions of the Gag polyprotein. *Curr. Top. Microbiol. Immunol.* **214,** 65–94.

Crawford, S., and Goff, S. (1984). Mutations in Gag proteins p12 and p15 of Moloney murine leukemia virus block early stages of infection. *J. Virol.* **49,** 909–917.

Fuller, S. D., Wilk, T., Gowen, B. E., Krausslich, H. G., and Vogt, V. M. (1997). Cryo-electron microscopy reveals ordered domains in the immature HIV-1 particle. *Curr. Biol.* **7**(10), 729–738.

Gamble, T. R., Yoo, S., Vajdos, F. F., Schwedler, U. K. v., Worthylake, D. K., Wang, H., McCutcheon, J. P., Sundquist, W. I., and Hill, C. P. (1997). Structure of the carboxyl-terminal dimerization domain of the HIV-1 capsid protein. *Science* **278,** 849–853.

Ganser, B. K., Li, S., Klishko, V. Y., Finch, J. T., and Sundquist, W. I. (1999). Assembly and analysis of conical models for the HIV-1 core. *Science* **283**(5398), 80–83.

Gorelick, R., Henderson, L., Hanser, J., and Rein, A. (1988). Point mutants of Moloney murine leukemia virus that fail to package viral RNA: Evidence for a specific RNA recognition by a "zinc finger-like" protein sequence. *Proc. Natl. Acad. Sci. USA* **85,** 8420–8424.

Hansen, M., Jelinek, L., Jones, R. S., Stegeman-Olsen, J., and Barklis, E. (1993). Assembly and composition of intracellular particles formed by Moloney murine leukemia virus. *J. Virol.* **67,** 5163–5174.

Hansen, M., Jelinek, L., Whiting, S., and Barklis, E. (1990). Transport and assembly of Gag proteins into Moloney murine leukemia virus particles. *J. Virol.* **64,** 5306–5316.

Hansen, M. S. T., and Barklis, E. (1995). Structural interaction between retroviral Gag proteins examined by cysteine cross-linking. *J. Virol.* **69**(2), 1150–1159.

Jin, Z., Jin, L., Peterson, D. L., and Lawson, C. L. (1999). Model for lentivirus capsid core assembly based on crystal dimers of EIAV p26. *J. Mol. Biol.* **286**(1), 83–93.

Jones, T. A., Blaug, G., Hansen, M., and Barklis, E. (1990). Assembly of Gag-β-galactosidase proteins into retrovirus particles. *J. Virol.* **64,** 2265–2279.

Kovari, L. C., Momany, C. A., Miyagi, F., Lee, S., Campbell, S., Vuong, B., Vogt, V. M., and Rossmann, M. G. (1997). Crystals of Rous sarcoma virus capsid protein show a helical arrangement of protein subunits. *Virology* **238,** 79–84.

Laemmli, U. K. (1970). Cleavage of structural proteins during the assembly of the head of bacteriophage T4. *Nature* **227,** 680–685.

Lobel, L. I., and Goff, S. P. (1984). Construction of mutants of Moloney murine leukemia virus by suppressor-linker insertional mutagenesis: Positions of viable insertion mutations. *Proc. Natl. Acad. Sci. USA* **81,** 4149–4153.

Mammano, F., Ohagen, A., Hoglund, S., and Gottlinger, H. G. (1994). Role of the major homology region of human immunodeficiency virus type one in virion morphogenesis. *J. Virol.* **68,** 4927–4936.

Maniatis, T., Fritsch, E. F., and Sambrook, J. (1982). "Molecular Cloning: A Laboratory Manual." Cold Spring Harbor Laboratory Press, Cold Spring Harbor, NY.

Mann, R., Mulligan, R., and Baltimore, D. (1983). Construction of a retrovirus packaging mutant and its use to produce helper-free defective retrovirus. *Cell* **33,** 153–159.

McDermott, J., Farrell, L., Ross, R., and Barklis, E. (1996). Structural analysis of human immunodeficiency virus type 1 Gag protein interaction using cysteine-specific reagents. *J. Virol.* **70**(8), 5106–5114.

Momany, C., Kovari, L. C., Prongay, A. J., Keller, W., Gitti, R. K., Lee, B. M., Gorbalenya, A. E., Tong, L., McClure, J., Ehrlich, L. S., Summers, M. F., Carter, C., and Rossman, M. G. (1996). Crystal structure of dimeric HIV-1 capsid protein. *Nat. Struct. Biol.* **3**(9), 763–770.

Ott, D. E., Coren, L. V., Kane, B. P., Busch, L. K., Johnson, D. G., Sowder, R. C. n., Chertova, E. N., Arthur, L. O., and Henderson, L. E. (1996). Cytoskeletal proteins inside human immunodeficiency virus type 1 virions. *J. Virol.* **70**(11), 7734–7743.

Ott, D. E., Hewes, S. M., Alvord, W. G., Henderson, L. E., and Arthur, L. O. (1998). Inhibition of Friend virus replication by a compound that reacts with the nucleocapsid zinc finger: Anti-retroviral effect demonstrated in vivo. *Virology* **243,** 283–292.

Pakula, A. A., and Simon, M. I. (1992). Determination of transmembrane structure by disufide cross-linking: The *Escherichia coli* Tar receptor. *Proc. Natl. Acad. Sci. USA* **89,** 4144–4148.

Pepinsky, R. (1983). Localization of lipid–protein and protein–protein interactions within the murine retrovirus gag precursor by a novel peptide-mapping technique. *J. Biol. Chem.* **258**(18), 11229–11235.

Pepinsky, R. B., Cappiello, D., Wilkowski, C., and Vogt, V. M. (1980). Chemical crosslinking of proteins in avian sarcoma and leukemia viruses. *Virology* **102,** 205–210.

Perrin-Tricaud, C., Davoust, J., and Jones, I. M. (1999). Tagging the human immunodeficiency virus gag protein with green fluorescent

protein. Minimal evidence for colocalisation with actin. *Virology* **255,** 20–25.

Pinter, A., and Fleissner, E. (1979). Structural studies of retroviruses: Characterization of oligomeric complexes of murine and feline leukemia virus envelope and core components formed upon cross-linking. *J. Virol.* **30**(1), 157–165.

Reicin, A., Paik, S., Berkowitz, R. D., Luban, J., Lowy, I., and Goff, S. P. (1995). Linker insertion mutations in the HIV-1 gag gene: Effects on virion particle assembly, release, and infectivity. *J. Virol.* **69,** 642–650.

Rein, A., Ott, D. E., Mirro, J., Arthur, L. O., Rice, W., and Henderson, L. E. (1996). Inactivation of murine leukemia virus by compounds that react with the zinc finger in the viral nucleocapsid protein. *J. Virol.* **70**(8), 4966–4972.

Rein, A., Ott, D. E., Mirro, J., Arthur, L. O., Rice, W. G., and Henderson, L. E. (1997). Suppression of retrovirial replication: Inactivation of murine leukemia virus by compounds reacting with the zinc finger in the viral nucleocapsid protein. *Leukemia* **11**(3), 106–108.

Rey, O., Canon, J., and Krogstad, P. (1996). HIV-1 Gag protein associates with F-actin present in microfilaments. *Virology* **220,** 530–534.

Scarlata, S., Ehrlich, L. S., and Carter, C. A. (1998). Membrane-induced alterations in HIV-1 Gag and matrix protein–protein interactions. *J. Mol. Biol.* **277**(2), 161–169.

Schwedler, U. K. V., Stemmler, T. L., Klishko, V. Y., Li, S., Albertine, K. H., Davis, D. R., and Sundquist, W. I. (1998). Proteolytic refolding of the HIV-1 capsid protein amino-terminus facilitates viral core assembly. *EMBO J.* **17**(6), 1555–1568.

Shinnick, T., Lerner, R., and Sutcliffe, J. (1981). Nucleotide sequence of Moloney murine leukemia virus. *Nature* **293,** 543–548.

Smyth, D. G., Blumenfeld, O. O., and Konigsberg, W. (1964). Reactions of *N*-ethylmaleimide with peptides and amino acids. *Biochem. J.* **91,** 589–595.

Stephenson, J., Tronick, S., and Aaronson, S. (1975). Murine leukemia virus mutants with temperature-sensitive defects in precursor processing cleavage. *Cell* **6,** 543–548.

Strambio-de-Castillia, C., and Hunter, E. (1992). Mutational analysis of the major homology region of Mason–Pfizer monkey virus by use of saturation mutagenesis. *J. Virol.* **66,** 7021–7032.

Swanstrom, R., and Wills, J. W. (1997). Synthesis, assembly, and processing of viral proteins. *In* "Retroviruses" (J. M. Coffin, S. H. Hughes, and H. E. Varmus, Eds.), pp. 263–334. Cold Spring Harbor Laboratory Press, Plainview, NY.

Tam, J. P., Wu, C.-R., Liu, W., and Zhang, J.-W. (1991). Disulfide bond formation in peptides by dimethyl sulfoxide. Scope and applications. *J. Am. Chem. Soc.* **113,** 6657–6662.

Wang, C.-T., Stegeman-Olsen, J., Zhang, Y., and Barklis, E. (1994). Assembly of HIV GAG-β-galactosidase fusion proteins into virus particles. *J. Virol.* **200,** 524–534.

Weiss, R., Teich, N., Varmus, H., and Coffin, J. (1984). "RNA Tumor Viruses," 2nd ed. Cold Spring Harbor Laboratory Press, Cold Spring Harbor, NY.

Weldon, R. A. J., and Wills, J. W. (1993). Characterization of a small (25-kilodalton) derivative of the Rous sarcoma virus Gag protein competent for particle release. *J. Virol.* **67,** 5550–5561.

Wilk, T., Gowen, B., and Fuller, S. D. (1999). Actin associates with the nucleocapsid domain of the human immunodeficiency virus Gag polyprotein. *J. Virol.* **73**(3), 1931–1940.

Wills, J. W., Cameron, C. E., Wilson, C. B., Xiang, Y., Bennet, R. P., and Leis, J. (1994). An assembly domain of the Rous sarcoma virus Gag protein required late in budding. *J. Virol.* **68,** 6605–6618.

Yang, Y. C., Ciarletta, A. B., Temple, P. A., Chung, M. P., Kovacic, S., Witek-Giannotti, J. S., Leary, A. C., Kriz, R., and Clark, S. C. (1986). Human IL-3 (multi-CSF): Identification by expression cloning of a novel hematopoietic growth factor related to murine IL-3. *Cell* **47,** 3–10.

Yeager, M., Wilson-Kubalek, E. M., Weiner, S. G., Brown, P. O., and Rein, A. (1998). Supramolecular organization of immature and mature murine leukemia virus revealed by electron cryo-microscopy: Implications for retroviral assembly mechanisms. *Proc. Natl. Acad. Sci. USA* **95**(13), 7299–7304.